Sensitive and real-time determination of H_2O_2 release from intact peroxisomes

Sebastian MUELLER*[1], Angelika WEBER*, Reiner FRITZ*, Sabine MÜTZE*, Daniel ROST*, Henning WALCZAK†, Alfred VÖLKL‡ and Wolfgang STREMMEL*

*Department of Internal Medicine IV, University of Heidelberg, Bergheimer Strasse 58, 69115 Heidelberg, Germany, †Division of Apoptosis Regulation, Tumor Immunology Program, German Cancer Research Center (DKFZ), 69120 Heidelberg, Germany, and ‡Institute of Anatomy and Cell Biology, University of Heidelberg, Im Neuenheimer Feld, 69120 Heidelberg, Germany

Peroxisomes are essential and ubiquitous cell organelles having a key role in mammalian lipid and oxygen metabolism. The presence of flavine oxidases makes them an important intracellular source of H_2O_2: an obligate product of peroxisomal redox reactions and a key reactive oxygen species. Peroxisomes proliferate in response to external signals triggered by peroxisome-proliferator-activated receptor signalling pathways. Peroxisome-derived oxidative stress as a consequence of this proliferation is increasingly recognized to participate in pathologies ranging from carcinogenesis in rodents to alcoholic and non-alcoholic steatosis hepatitis in humans. To date, no sensitive approach exists to record H_2O_2 turnover of peroxisomes in real time. Here, we introduce a sensitive chemiluminescence method that allows the monitoring of H_2O_2 generation and degradation in real time in suspensions of intact peroxisomes. Importantly, removal, as well as release of, H_2O_2 can be assessed at nanomolar, non-toxic concentrations in the same sample. Owing to the kinetic properties of catalase and oxidases, H_2O_2 forms fast steady-state concentrations in the presence of various peroxisomal substrates. Substrate screening suggests that urate, glycolate and activated fatty acids are the most important sources for H_2O_2 in rodents. Kinetic studies imply further that peroxisomes contribute significantly to the β-oxidation of medium-chain fatty acids, in addition to their essential role in the breakdown of long and very long ones. These observations establish a direct quantitative release of H_2O_2 from intact peroxisomes. The experimental approach offers new possibilities for functionally studying H_2O_2 metabolism, substrate transport and turnover in peroxisomes of eukaryotic cells.

Key words: catalase, lipid metabolism, oxidative stress, peroxisome proliferation, redox regulation.

INTRODUCTION

Peroxisomes are subcellular, single, membrane-bound respiratory organelles that are present in virtually all eukaryotic cells, and carry out a wide range of essential functions, including β-oxidation of fatty acids, biosynthesis of plasmalogens, cholesterol, bile acids, glyoxylate metabolism, and metabolism of reactive oxygen species [1]. Glyoxysomes are their counterparts in plants, and have a similar role in β-oxidation and glyoxylate metabolism [2,3].

In humans, defects in structure or function of peroxisomes give rise to a group of genetically distinct, mostly fatal, inborn errors: the peroxisomal disorders [4]. Besides these rare hereditary diseases, peroxisomes proliferate in the presence of non-genotoxic chemicals that lead to carcinogenesis in rodents [5,6]. Peroxisome proliferators include a wide range of chemicals, such as phthalate esters and thrichlorethylene herbicides, but also epidemiologically important drugs or compounds such as ethanol, hypolipidaemic drugs and hormones. These structurally diverse compounds produce similar pleiotropic effects in the peroxisomal compartment, a differential increase in peroxisomal enzymes and hepatocarcinogenesis in rats and mice. Further studies have led to the discovery of peroxisome-proliferator-activated receptors ('PPARs') that mediate peroxisomal hyperplasia and proliferation; however, the precise mechanism of carcinogenesis in rodents is not well understood [6,7]. Moreover, peroxisomes are increasingly considered to be involved in common human pathologies, such as alcoholic and non-alcoholic steatosis hepatitis [8–10].

Peroxisome-derived oxidative stress has long been under debate in mediating at least some of the consequences of peroxisomal proliferation [11,12]. Peroxisomes have been characterized initially by the presence of several H_2O_2-generating flavine oxidases, together with H_2O_2-degrading catalase. In contrast with mitochondria, peroxisomal β-oxidation is not coupled with oxidative phosphorylation. Rather, oxygen is stoichiometrically converted into H_2O_2, and peroxisomes have been estimated to consume between 10–30% of the oxygen consumed by the liver [13]. Assuming an efficient interplay of β-oxidation enzymes and catalase during the breakdown of fatty acids, oxygen is reduced to water and the energy is dissipated in the form of heat. If catalase is not efficient in trapping H_2O_2, it may escape from peroxisomes. The morphological and biochemical changes that occur during peroxisomal proliferation are thought to result from such an increase in the synthesis of H_2O_2 without a concomitant increase in the capacity of its degradation by catalase, which, in turn, leads to DNA damage and eventually neoplasia [12].

Besides their toxicity [14] and well-established physiological functions in synthetic pathways and phagocytosis, reactive oxygen species are considered to be potential signalling molecules, and the study of redox regulation has emerged as a broad and expanding field [15–18]. Consequently, peroxisome-derived H_2O_2 might not solely act as a DNA-damaging agent, but might rather modulate signalling cascades involved in cell proliferation or apoptosis. Indeed, the redox-sensitive transcription factor nuclear factor κB (NF-κB) [19] is activated in the presence of peroxisome proliferators, and this activation can be simulated by

Abbreviation used: NF-κB, nuclear factor κB.

[1] To whom correspondence should be addressed (e-mail sebastian.mueller@urz.uni-heidelberg.de).

overexpression of the H_2O_2-generating acyl-CoA oxidase, which is the first enzyme of the peroxisomal β-oxidation pathway [20].

One of the major difficulties in the direct measurement of peroxisomal H_2O_2 metabolism has been the lack of an appropriate analytical tool. Additionally, no method is known to date that allows the direct determination and comparison of both catalase and oxidase activities in intact peroxisomes at non-toxic (i.e. physiological) H_2O_2 concentrations. Using a sensitive chemiluminescence assay [21,22], we establish in the present study a procedure that permits the real-time determination of H_2O_2 generation and degradation in intact liver peroxisomes. Importantly, studies were performed at H_2O_2 concentrations that are found *in vivo*. We demonstrate that H_2O_2 is released from peroxisomes in the presence of various peroxisomal substrates. A steady-state concentration of H_2O_2 is formed under these conditions. The kinetic screening with several peroxisomal substrates shows that urate, glycolate and activated fatty acids are most efficient in producing H_2O_2. The data suggest further that peroxisomes are an important site for medium-length fatty acid β-oxidation.

MATERIALS AND METHODS

Chemicals

Luminol, catalase, glucose oxidase, H_2O_2, sodium hypochlorite and sodium azide were obtained from Sigma (Deisenhofen, Germany). Acyl-CoA esters and other peroxisomal substrates, such as palmitoyl-CoA, lignoceryl-CoA, octanoyl-CoA, palmitoleoyl-CoA, arachidonoyl-CoA, stearoyl-CoA, urate, glycolate, spermidine, heptadecanoyl-CoA, pentadecanoyl-CoA, proline and alanine, were likewise from Sigma.

Solutions

Stock solutions of luminol were prepared in 10 mM PBS and adjusted to pH 7.4. Stock solutions of sodium hypochlorite and H_2O_2 were prepared in water. Their concentrations were determined spectrophotometrically (ϵ_{290} 350 litre · mol^{-1} · cm^{-1} at pH 12 [23] and ϵ_{230} 74 litre · mol^{-1} · cm^{-1} [24] for sodium hypochlorite and H_2O_2 respectively). Solutions of sodium hypochlorite and H_2O_2 were freshly prepared, and PBS/Dulbecco (137 mM NaCl/2.7 mM KCl/8.1 mM Na_2HPO_4/1.48 mM KH_2PO_4/0.49 mM $MgCl_2.6H_2O$/0.9 mM $CaCl_2$) was used as the phosphate buffer. Fresh preparations of peroxisomes were suspended in a buffer adjusted to pH 7.4 containing 250 mM sucrose, 5 mM Mops, 1 mM EDTA and 0.5% (v/v) ethanol.

Isolation of peroxisomes

Peroxisomes were isolated from the liver of Wistar rats using the metrizamide gradient technique, as described previously [25]. This method yields intact peroxisomes with a high degree of purity (approx. 98%; [25]). To verify the results further, very pure peroxisomal preparations were obtained using the recently described technique of immune free-flow electrophoresis [26]. Suspensions of isolated peroxisomes were washed in PBS to remove extra-peroxisomal catalase, which is known to leak from peroxisomes during preparation [27]. The washing protocol included a step of washing once with PBS for 5 min at 8000 rev./min and then washing three times for 5 min at 5000 rev./min. Figure 1(a) shows the efficient removal of matrix enzymes (catalase and acyl-CoA oxidase) from the supernatant during the washing cycles. Coomassie Blue staining of pellets and supernatants demonstrates further that some catalase has leaked from the original peroxisome preparation, whereas no urate oxidase is detected in the first supernatant (Figure 1b). Already, the second supernatant contains urate oxidase and much less catalase. This finding is indicative of small but intact peroxisomes that are not pelleted under these centrifugation conditions. After

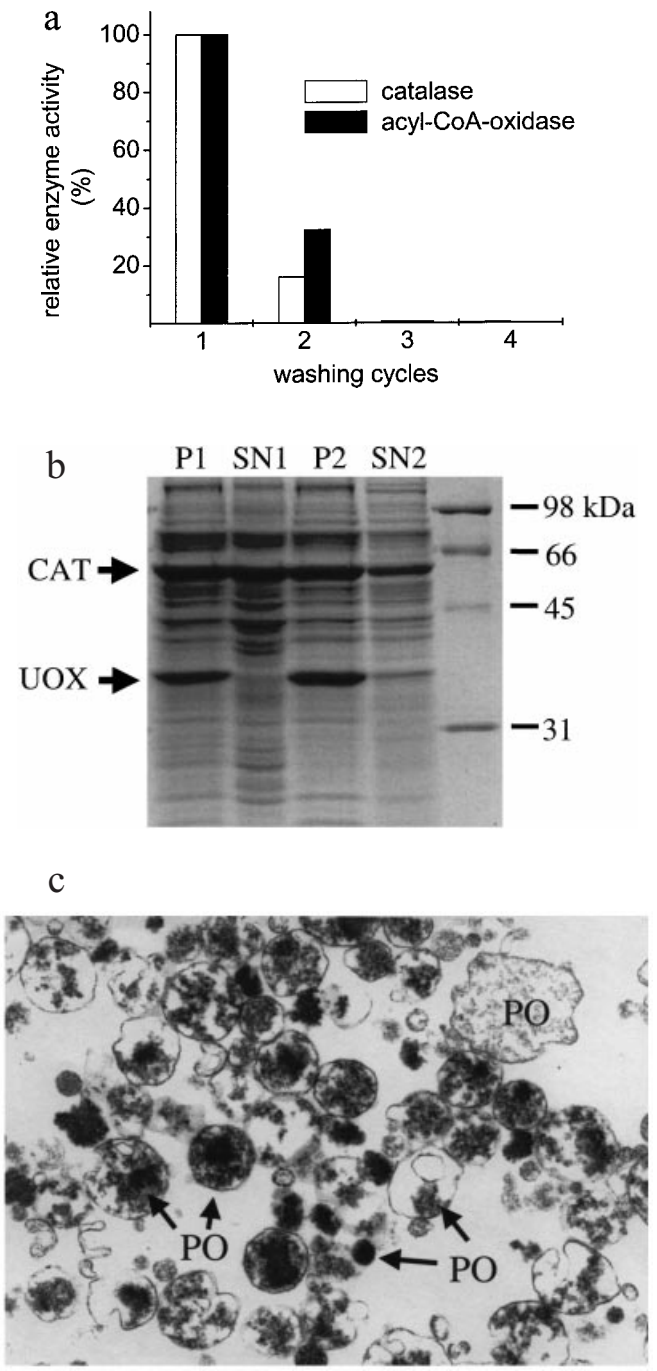

Figure 1 Preparation of highly purified intact peroxisomes from rat liver that are free of leaked matrix enzymes

To remove leaked catalase, isolated peroxisomes were further washed in PBS in four subsequent washing steps. (**a**) The efficient removal of catalase and acyl-CoA oxidase by determining the remaining enzyme activities in the supernatant. (**b**) Coomassie Blue-stained gel of the first and second pellet (P1 and P2) and supernatant (SN1 and SN2). Abundance of catalase and absence of urate oxidase clearly indicate that the initial supernatant SN1 is the major source of leaked catalase. In (**c**), a representative electron micrograph confirms that the washing procedure yields morphologically intact and heterogeneous peroxisomes of different size (DAB; ×18000). PO, peroxisomes.

four washing cycles, the peroxisome preparation is free from leaked matrix enzymes and the peroxisomes are found to be morphologically intact as demonstrated in the electron micrograph (Figure 1c). Catalase and oxidase activities in the supernatant of peroxisome preparations were measured using a recently described sensitive chemiluminescence technique [22,28]. Lysates of peroxisomes were prepared in the presence of 0.01 % (w/v) Triton X-100. This concentration allowed an almost-complete lysis of peroxisomal membranes, without inactivation of oxidases (results not shown). Protein concentrations of peroxisome preparations were determined using the Bradford method.

SDS/PAGE

SDS/PAGE was performed under reducing conditions, with 12.5 % (w/v) acrylamide gels [29]. Samples were boiled for 5 min in sample buffer, approx. 10 μg of protein was loaded per lane, and these were then electrophoresed at a constant current of 25 mA. Gels were stained with Coomassie Blue.

Electron microscopy

Aliquots of fractions were mixed with one-half of their volume of an ice-cold fixative containing 7.5 % (v/v) glutaraldehyde. After fixation for 30 min at 4 °C, the fractions were diluted with 2.5 % glutaraldehyde in PBS buffer to a final concentration of 150 μg of protein/ml, and filtered at a pressure of 10^5 Pa through Millipore membranes with a pore size of 25 μm and a diameter of 13 mm. The preparations were incubated for 30 min in the alkaline DAB medium for cytochemical localization of catalase [30], followed by post-fixation in 2 % (w/v) aqueous osmium tetroxide. All material was dehydrated in graded ethanol solutions and embedded in Epon. Ultra-thin sections were cut with a diamond knife on an ultramicrotome, contrasted with uranyl acetate and lead citrate, and examined under a Philips 301 electron microscope.

Determination of steady-state H_2O_2 concentrations, catalase and oxidase activities

H_2O_2 was determined using the luminol-hypochlorite assay, as described previously [21,22]. A flow technique was established to follow rapid kinetics of catalase and oxidases in real time [22,28,31]. Briefly, solutions of isolated catalase or glucose oxidase and diluted suspensions of intact or lysed peroxisomes were aspirated via a peristaltic pump (4 ml/min). Luminol (10^{-4} M) and hypochlorite (10^{-4} M) were continuously added by a perfusor pump (12 ml/min) to the sample solution. Chemiluminescence intensities were measured in intervals of 1 s in the reaction flow chamber using a computer-driven AutoLumat LB953 (Berthold, Wildbad, Germany). The AutoLumat was used for all luminescence determinations and programs were written in GW Basic. Continuous magnetic stirring was used to ensure a rapid mixing of the enzyme substrate solution. Temperature was maintained at 22 °C. The assay was calibrated with 10 μM H_2O_2 (final concentration). Background luminescence was defined as the remaining luminescence intensities in the absence of H_2O_2 (in the presence of catalase), and finally subtracted from the luminescence intensity data.

Since catalase is not saturable by its substrate H_2O_2 and does not follow Michaelis–Menten kinetics, no value for V_{max} can be determined under saturation conditions. Therefore catalase activity is obtained by determining the exponential decay constant of the catalase-mediated H_2O_2 degradation using linear-regression analysis. The activity is given in units of s^{-1} [28,32]. Rates of H_2O_2 generation by oxidases are intentionally expressed as mol of $H_2O_2 \cdot s^{-1}$, instead of μmol · min^{-1} or international units (i.u.) to facilitate calculation of H_2O_2 steady-state concentrations using the equation $[H_2O_2]_{ss} = k_{ox}/k_{cat}$, where $[H_2O_2]_{ss}$ is the steady-state H_2O_2 concentration, k_{ox} is the oxidase activity and k_{cat} is the catalase activity. In addition, oxidase activities were measured for various oxidase substrate concentrations (e.g. urate, glucose, palmitoyl-CoA) at a constant oxygen concentration of 250 μM and at 22 °C. To establish a peroxisomal model with respect to H_2O_2 generation and removal, a mixture of purified glucose oxidase and bovine liver catalase was used. The stock solution of glucose oxidase (G-9010, 200 units · mg of protein $^{-1}$; Sigma) was found to generate 2.3×10^{-3} M $H_2O_2 \cdot s^{-1}$ at 22 °C in the presence of 5 mM glucose and in air-saturated PBS (250 μM oxygen). Catalase activity of the catalase stock solution (C-3155; Sigma) was determined to be 1195 s^{-1}. Regression analysis was performed using Origin Software Version 6.0 (Microcal Software, Inc., Northampton, MA, U.S.A.). To obtain Lineweaver–Burk plots, steady-state H_2O_2 concentrations in suspensions of peroxisomes or a solution of catalase/glucose oxidase were examined further using the injection modus of the luminol-hypochlorite assay [22]. Briefly, 1 ml sample solutions were incubated with 5×10^{-5} M luminol. Upon reaching a steady-state concentration of H_2O_2, 50 μl of sodium hypochlorite (1 μM final concentration) was added, and the short luminescence signal was determined immediately using the AutoLumat LB953-integrated injection device in measuring position and an integration time of 2 s. Calibration was performed using batches with known H_2O_2 concentrations of 5 μM. Background luminescence was determined in the absence of H_2O_2, and finally subtracted. It is important to mention that the luminol-hypochlorite assay does not detect H_2O_2 within cells and organelles [22].

RESULTS

Determination of H_2O_2 removal (catalase) and H_2O_2 generation (oxidase) in a mixture of purified glucose oxidase and catalase

It is not known whether, or to what extent, peroxisomes contribute to intracellular oxidative stress and redox-sensitive cell regulation. In order to establish the prime objective of measuring generation and removal of H_2O_2 in peroxisomes, we first studied a model of peroxisomes with respect to H_2O_2 metabolism by using a mixture of purified catalase and glucose oxidase. In this model, the purified catalase represents the intra-peroxisomal catalase, whereas glucose oxidase is a representative of one of the many peroxisomal oxidases.

First, enzyme activities were determined separately. Figure 2(a) shows a semi-logarithmic plot of the exponential decay of H_2O_2 with purified bovine liver catalase (1:33000) using the sensitive luminol-hypochlorite assay in real time. The kinetics of the exponential decay are typical for catalase, since the enzyme is not saturable up to molar H_2O_2 concentrations. Therefore determination of K_m is impossible and catalase activity is usually given by the rate constant (k) in the equation $k_{cat} = \ln([S_1]/[S_2])/dt$, where dt is the measured time interval and $[S_1]$ and $[S_2]$ are H_2O_2 concentrations at time t_1 and t_2 respectively [28,32]. Using linear regression analysis, the rate constants were determined with high accuracy ($r^2 > 0.99$). As is demonstrated further in Figure 2(a), catalase is inhibited by the addition of sodium azide, a competitive catalase inhibitor (denoted by the second arrow). Owing to this inhibition, an almost undetectable catalase activity ($k = 1.5 \times 10^{-4}$ s^{-1}) remains. The slight increase in H_2O_2 concentration after addition of sodium azide is due to a low level of contamination by H_2O_2.

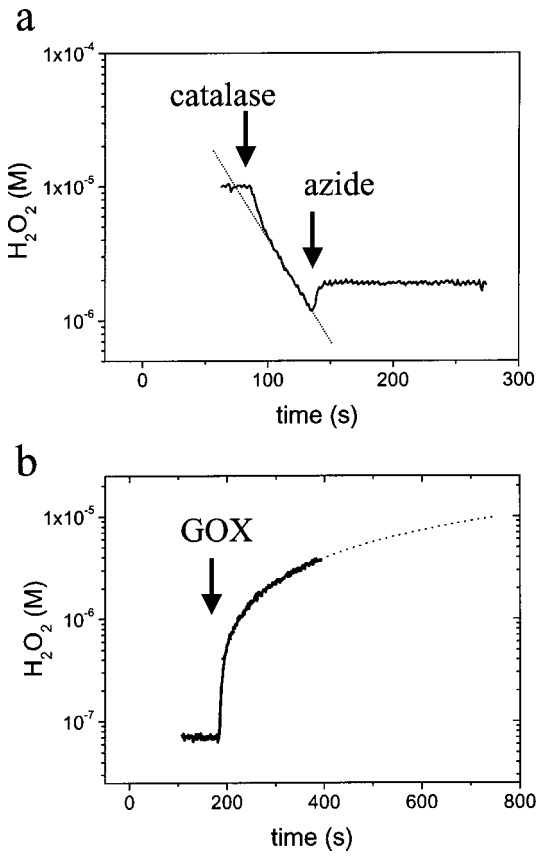

Figure 2 Exponential degradation of H_2O_2 by isolated bovine liver catalase (a), and generation of H_2O_2 by isolated glucose oxidase (b)

Isolated liver catalase (1:33 000) is added into an H_2O_2 solution and decay was measured in real time using the luminol-hypochlorite system [22]. Addition of 1 mM sodium azide, a competitive catalase inhibitor, inhibits catalase by 99%. Dotted lines represent the linear regression analysis curves. Catalase activity is 3.6×10^{-2} s^{-1} before, and 1.5×10^{-4} s^{-1}, after inhibition with azide. The experiment shown is representative of three independent determinations. Addition of glucose oxidase (1:150 000) into a PBS-buffered glucose solution (5 mM) causes rapid increase of H_2O_2. In this semi-logarithmic plot, the generation of H_2O_2 follows pseudo-zero-order kinetics ($r^2 > 0.99$), with k_{GOX} (the catalytic rate of glucose oxidase) = 1.6×10^{-8} M · s^{-1}. The depicted experiment is representative of three independent determinations.

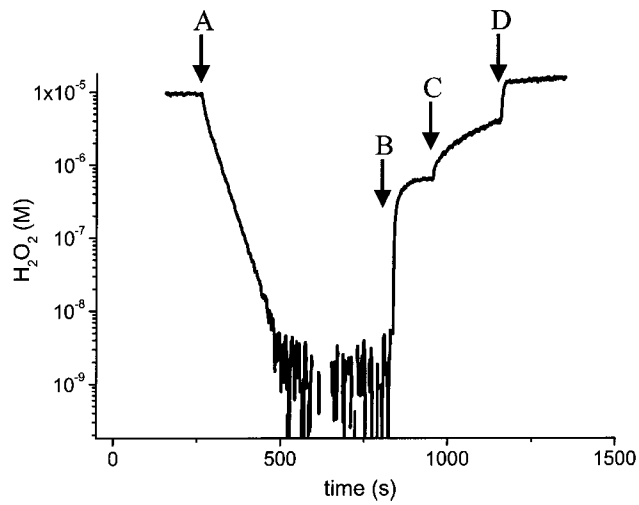

Figure 3 Real-time determination of catalase and glucose oxidase activity in a mixture of both purified catalase and glucose oxidase mimicking peroxisomes with respect to H_2O_2 metabolism

Enzyme addition at time point A [dilutions of 1:33 000 (catalase) and 1:150 000 (glucose oxidase)] was followed by the catalase-mediated exponential decay of H_2O_2. A steady-state equilibrium of H_2O_2 is reached after addition of 5 mM glucose (time point B) as a consequence of both H_2O_2 removal and generation. In the presence of 1 mM sodium azide (time point C) catalase is inhibited, and H_2O_2 can accumulate. Inhibition of catalase is demonstrated by the final addition of 10 μM H_2O_2. Catalase activity ($k_{cat} = 3.6 \times 10^{-2}$ s^{-1}) and glucose oxidase activity ($k_{gox} = 1.7 \times 10^{-8}$ M H_2O_2 · s^{-1}) are in excellent agreement with the results obtained in solutions of isolated enzymes (see Figure 2). The depicted experiment is representative of three independent determinations.

In Figure 2(b), the generation of H_2O_2 by purified glucose oxidase (GOX in the Figure) is measured. Glucose oxidase reduces oxygen to H_2O_2 using glucose as a substrate, and this reaction follows a Ping-Pong mechanism-type kinetics [33]. After addition of glucose oxidase (1:150000 dilution), H_2O_2 is formed rapidly. Under these conditions, oxygen and glucose concentrations remained almost unchanged, allowing a pseudo-zero-order generation rate of H_2O_2, as demonstrated by linear regression analysis. A semi-logarithmic plot was used to identify the zero-order nature of the kinetics, and to compare more easily the differences in catalase and oxidase kinetics over a broad concentration range.

We then set about establishing a procedure to determine enzyme activities in a mixture of purified catalase and glucose oxidase that represents a peroxisome model with respect to H_2O_2 metabolism. Previous studies on human erythrocytes had shown that two enzymes can be determined sequentially with the luminol-hypochlorite technique [31]. In Figure 3, the assay was first calibrated with 10 μM H_2O_2. At time point A, a mixture of purified glucose oxidase and catalase was added using the same enzyme concentrations as those described above for Figure 2. An exponential catalase-mediated decay of H_2O_2 was observed down to nanomolar concentrations and, importantly, the activity does not differ from the values obtained in Figure 2(a). At these very low H_2O_2 concentrations, the background noise increased, as demonstrated in the semi-logarithmic plot. At time point B, addition of 5 mM glucose was followed by a rapid increase in H_2O_2. Owing to the presence of both glucose oxidase and catalase, a steady-state level of H_2O_2 was formed that could be maintained over a long time. As reported earlier, the equilibrium of H_2O_2 decay by catalase and the H_2O_2 generation by glucose oxidase was obtained at $k_{gox} = k_{cat} \cdot [H_2O_2]$ [34,35], where k_{gox} represents the rate of glucose oxidase activity. Assuming a constant glucose and oxygen concentration, steady-state H_2O_2 concentrations can be calculated as follows: $[H_2O_2] = k_{gox}/k_{cat}$. Thus the knowledge of both the activity of catalase and the steady-state concentration of H_2O_2 at the equilibrium allows the calculation of the oxidase activity. The calculated glucose oxidase activity ($k_{gox} = 1.7 \times 10^{-8}$ mol of H_2O_2 · s^{-1}) is in excellent agreement with the results obtained in solutions of isolated glucose oxidase (see Figure 2b). Inhibition of catalase by sodium azide at time point C apparently led to the accumulation of H_2O_2.

Determination of glucose oxidase activity for various substrate concentrations using the H_2O_2 steady-state approach

We have established a procedure that allows the sequential determination of catalase, as well as oxidase, activities in one sample at very low H_2O_2 concentrations (Figure 3). In Figure 3, steady-state equilibrium is reached within 150 s after the addition

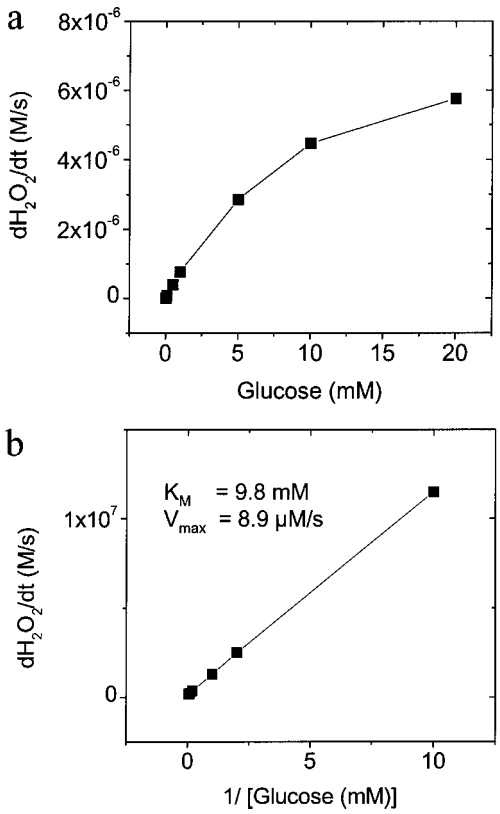

Figure 4 Determination of Michaelis–Menten plot (a) and Lineweaver–Burk plot (b) for glucose oxidase (glucose concentration measured against H_2O_2 generation rate) using steady-state end-point determinations of H_2O_2

Various amounts of glucose were added into a mixture of catalase and oxidase mimicking peroxisomes with respect to H_2O_2 metabolism. Steady-state concentrations of H_2O_2 were determined using the luminol-hypochlorite assay. All data points are the means for three independent experiments. Standard deviations are too small to be displayed in the Figure.

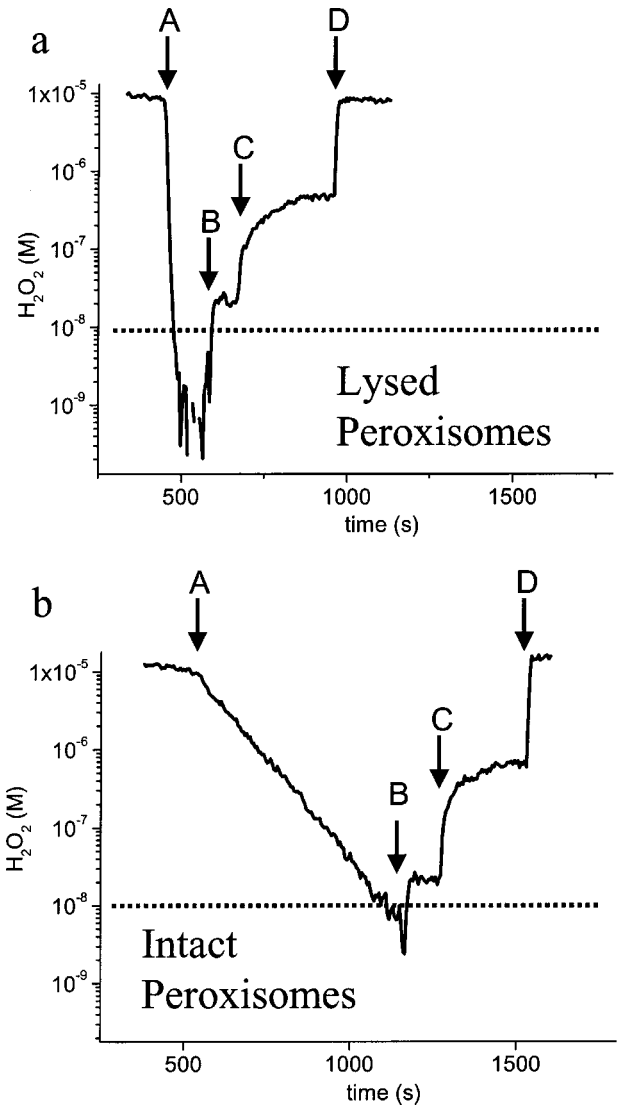

Figure 5 Sensitive and real-time determination of catalase and acyl-CoA oxidase activity in isolated lysed (a) and intact (b) rat liver peroxisomes at very low H_2O_2 concentrations

Addition of peroxisomes (time point A) is followed by the catalase-mediated exponential decay of H_2O_2. A steady-state equilibrium of H_2O_2 is reached after addition of 3 μM palmitoyl-CoA (final concentration) at time point B as a consequence of both H_2O_2 removal and generation. In the presence of 1 mM sodium azide (time point C) catalase is inhibited and H_2O_2 can accumulate. Inhibition of catalase is demonstrated by the final addition of 10 μM H_2O_2. The peroxisome suspension (10 mg/ml protein) was used in a 1:100 dilution. The steady-state concentrations of H_2O_2 are similar in lysed and intact peroxisomes. The catalase activity used in (**a**) was 0.18 s^{-1}; the steady-state concentration of H_2O_2 was 2.2×10^{-8} M H_2O_2, and the acy-CoA oxidase activity was 3.9×10^{-8} M · s^{-1}. Catalase activity in (**b**) was 0.011 s^{-1}; the steady-state concentration of H_2O_2 was 2.1×10^{-8} M H_2O_2 and the acyl-CoA oxidase activity was 3.8×10^{-8} M · s^{-1}. The depicted experiment is representative of three independent determinations and peroxisome preparations.

of glucose. Using this approach, the rate of H_2O_2 generation by glucose oxidase was determined in the presence of various glucose concentrations, and the resulting Michaelis–Menten plot is shown in Figure 4(a). K_m and V_{max} values were obtained from the Lineweaver–Burk plot shown in Figure 4(b).

Real-time determination of catalase and acyl oxidase activity in intact and lysed liver peroxisomes

Next, we applied the same procedure to isolated lysed peroxisomes from rat liver. Lysed peroxisomes were used because they lack compartmentalizing membranes and matrices, and resemble much more closely the biochemical model described above (Figures 2–4). Figure 5(a) shows a representative example of real-time determination of H_2O_2 degradation by catalase, and H_2O_2 generation by acyl oxidase in the presence of palmitoyl-CoA using highly diluted lysed peroxisomes.

The data follow the exact pattern as demonstrated for the catalase–glucose oxidase system. Additional experiments confirmed that H_2O_2 is specifically generated by acyl-CoA oxidase. Heat inactivation at 80 °C for 5 min completely abolished H_2O_2 production in the presence of palmitoyl-CoA. In the presence of palmitate, the non-activated fatty acid, no H_2O_2 generation is observed (results not shown). This is in agreement with the general fact that peroxisome acyl-CoA oxidases require the activation of fatty acids by CoA [36]. Mitochondrial contamination of our very pure peroxisome preparations does not contribute to the observed H_2O_2 generation: first, mitochondrial β-oxidation requires co-substrates that have not been added under our conditions. Secondly, only β-oxidation in peroxisomes is accompanied by H_2O_2 production. Indeed, inhibition of the respiratory chain by potassium cyanide did not affect H_2O_2 generation in our experiments (results not shown).

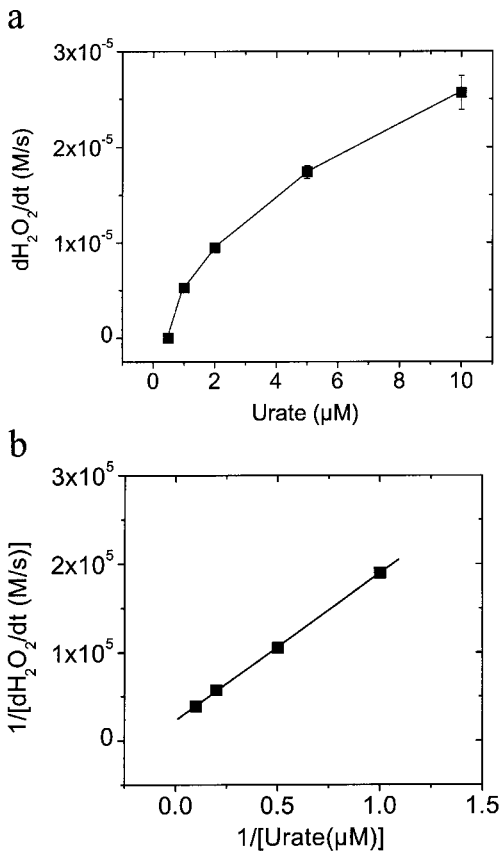

Figure 6 Michaelis–Menten plot (a) and Lineweaver–Burk plot (b) for urate oxidase (urate concentration measured against H_2O_2 generation rate) in fresh peroxisomes using steady-state end-point determinations of H_2O_2

Various amounts of urate were added into a solution of fresh lysed peroxisomes. Steady-state concentrations of H_2O_2 were determined using the luminol-hypochlorite assay. All data points are the means for three independent experiments. Where not indicated by error bars, the standard deviations are too small to be displayed in the Figure.

Table 1 K_m and V_{max} values of H_2O_2 generation for various substrates of peroxisome oxidases using the luminol-hypochlorite assay

Kinetic parameters correspond to a lysate of purified peroxisomes with 1 mg/ml protein. Corresponding catalase activity in this solution is determined to be 208 s^{-1}. Oxidase activities are deliberately given in M $H_2O_2 \cdot s^{-1}$ and not as μmol · min^{-1}, since the steady-state concentration of H_2O_2 can be determined directly from catalase and oxidase activities according to the eqn $[H_2O_2]_{ss} = k_{ox}/k_{cat}$ (see the Materials and methods section). Standard deviations are $< 10\%$.

Substrate	V_{max} (M $H_2O_2 \cdot s^{-1}$)	K_m (μM; substrate)
Acyl-CoA oxidase		
Octanoyl-CoA ($C_{8:0}$)	6.2×10^{-6}	39.1
Pentadecanoyl CoA ($C_{15:0}$)	2.5×10^{-6}	1.1
Palmitoyl-CoA ($C_{16:0}$)	2.4×10^{-6}	0.5
Palmitoleoyl-CoA ($C_{16:1}$)	3.1×10^{-6}	1.2
Heptadecanoyl-CoA ($C_{17:0}$)	1.9×10^{-6}	1.0
Stearoyl-CoA ($C_{18:0}$)	2.0×10^{-6}	1.1
Arachidonoyl-CoA ($C_{20:4}$)	1.5×10^{-6}	1.5
Lignoceryl-CoA ($C_{22:0}$)	5.6×10^{-7}	2.1
Other oxidases		
Urate	4.4×10^{-5}	7.3
Glycolate	4.2×10^{-6}	29.3
Spermidine	2.4×10^{-6}	9.2
D-Amino acid oxidase		
Proline	4.2×10^{-7}	11.3
Alanine	4.3×10^{-7}	1.7

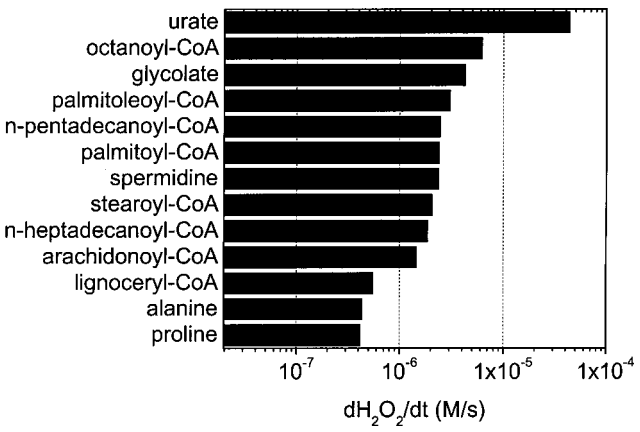

Figure 7 Maximum velocities of H_2O_2 generation (V_{max}) in descending order for various peroxisomal oxidases using isolated rat liver peroxisomes

H_2O_2 generation rates correspond to a protein concentration of 1 mg/ml. Corresponding catalase activity in this solution was determined to be 208 s^{-1}. Data were obtained from Lineweaver–Burk plots, as described in the legend to Figure 5. Standard deviations are $< 10\%$.

To assess whether this system can also be used for intact organelles, we then applied the H_2O_2 analysis to fresh and integral peroxisomes from rat liver. As is shown in Figure 5(b), intact peroxisomes have a similar response regarding catalase-mediated H_2O_2 degradation (time point A), H_2O_2 steady-state generation following addition of palmitoyl-CoA (time point B) and rapid accumulation of H_2O_2 after catalase inhibition (time point C). Complete inhibition of catalase is confirmed by a final addition of 10 μM H_2O_2 (time point D). Although the responses are comparable with the lysate in terms of quality, important quantitative differences are apparent. First, catalase-mediated decay of H_2O_2 is much slower, representing only 6.4% of the catalase activity of the lysed peroxisomes (Figure 5a). This so-called latency, or 'occluded' catalase activity, is considered to depend on diffusion of H_2O_2 into the peroxisome via membrane and peroxisomal matrices [27,37]. Thus the high catalase latency in our experiment confirms the functional and structural integrity of the peroxisomes [25].

Secondly, the result also shows that intact peroxisomes release H_2O_2 into the surroundings. Interestingly, the steady-state concentration of H_2O_2 is found to be almost identical in intact and lysed peroxisomes (2.2×10^{-8} compared with 2.1×10^{-8} M H_2O_2 respectively). These observations suggest that catalase does not completely prevent H_2O_2 release from intact peroxisomes. Moreover, peroxisomes are not very competent at removing H_2O_2 from the surroundings.

Generation of H_2O_2 by various peroxisomal substrates: maximum velocities and Michaelis–Menten constants

Using the steady-state endpoint determination of H_2O_2, we studied several substrates of peroxisomal oxidases to determine their efficiency in generating H_2O_2. As described in Figure 4 for the catalase–glucose oxidase system, Michaelis–Menten and

Lineweaver–Burk plots were obtained for these substrates. Representatively, both plots are shown in Figure 6 for urate oxidase, which we determined as the most efficient oxidase at generating H_2O_2 in rat liver peroxisomes. K_m and V_{max} values were calculated from the Lineweaver–Burk plots by linear regression analysis. Table 1 shows the kinetic data for all substrates. Figure 7 presents maximum velocities for these substrates in descending order, which reveals which substrates are highly efficient in generating H_2O_2. Urate is followed by a set of activated fatty acids together with glycolate. D-Amino acids are less efficient in contributing to H_2O_2 release. Interestingly, the medium-chain fatty acid octanoyl-CoA provides the highest generation rate for H_2O_2 among all the fatty acids that have been studied.

DISCUSSION

Peroxisomes are essential and ubiquitous organelles containing several flavine oxidases that reduce oxygen to H_2O_2. Despite the intra-peroxisomal abundance of catalase, which decomposes H_2O_2, peroxisome-derived oxidative stress is considered to have an important role in different pathologies, such as hepatocarcinogenesis in rodents, and liver inflammation, such as non-alcoholic steatosis hepatitis in humans. A series of experimental models have focused on the underlying mechanisms. First, conditions that produce peroxisome proliferation lead to an induction of β-oxidation enzymes, such as acyl-CoA oxidase, without a concomitant increase in catalase activity [12]. Secondly, overexpression of acyl oxidase activates the redox-sensitive transcription factor NF-κB, which can be abrogated in the presence of certain antioxidants [20,38]. Thirdly, a transformation in epithelial cells was observed when urate oxidase was stably transfected [39]. Fourthly, livers with chronic peroxisome proliferation show a 4-fold increase in the amount of 8-hydroxy-2′-deoxyguanosine in DNA, which is a typical 'fingerprint' of oxidative DNA damage [40,41]. In contrast with these indirect pieces of data, several lines of evidence are not in favour of this hypothesis. Oxidative damage could not be shown in the liver under conditions of peroxisomal proliferation [42] and, additionally, a possible escape of H_2O_2 has been questioned, given the high rate at which peroxisomal catalase converts H_2O_2 into water and oxygen [6]. One of the drawbacks in addressing these questions has been the lack of appropriate analytical tools in functionally studying H_2O_2 metabolism in intact peroxisomes.

Here, we show directly the release of H_2O_2 from intact liver peroxisomes in the presence of various substrates at nanomolar, non-toxic H_2O_2 concentrations using a novel, sensitive H_2O_2 assay [22]. A steady-state concentration of H_2O_2 is rapidly formed in the presence of various peroxisomal substrates. Most importantly, H_2O_2 decomposition by catalase and H_2O_2 generation by oxidases can be measured in real time. For the first time, this new experimental approach allows the direct determination of imbalances in peroxisomal H_2O_2 metabolism.

The new procedure offers three main advantages. First, catalase and oxidase are determined in the same sample using the original quantitative ratio of both enzymes. Thus small changes in the ratio of both enzymes can be detected that have been proposed to have a crucial role in peroxisome-derived oxidative stress. On a methodological note, neither of the enzymes are inactivated under these low H_2O_2 concentrations; nor is molecular oxygen released in a gaseous form that could lead to severe artefacts [28]. Moreover, these H_2O_2 concentrations are below or within the range that may occur *in vivo* and that that may trigger signalling pathways [43,44].

Secondly, removal of H_2O_2 in the initial stage drastically enhances the sensitivity towards even the lowest levels of release of H_2O_2 by oxidases. This is also important, because small traces of 10^{-8}–10^{-7} M H_2O_2 are known to be present in aqueous solutions [22].

Thirdly, the procedure allows the direct determination of the real steady-state concentration of H_2O_2 that is provided by the equation $[H_2O_2]_{ss} = k_{ox}/k_{cat}$. Using this equation, oxidase activity can readily be calculated from the catalase activity and steady-state H_2O_2 concentration. This latter approach avoids the usage of inhibitors (e.g. azide) that might interfere with the enzymes. In addition, the measuring time is minimized, and various substrates can be determined in a short time, which is especially useful, since fresh peroxisome preparations rapidly change their biochemical properties within hours.

Our studies on intact and lysed rat liver peroxisomes mainly address three biochemical phenomena of peroxisomes. First, catalase latency is demonstrated in the real time, since intact peroxisomes remove H_2O_2 at a much lower rate than the corresponding lysate. Catalase latency has been known for a long time and it is usually ascribed to the rate-limiting diffusion of H_2O_2 through biomembranes [28,37,45]. However, no difference was found between the palmitoyl-CoA-mediated steady-state H_2O_2 generation of intact and lysed peroxisomes. These findings suggest that peroxisomes remove intra-peroxisomal-derived H_2O_2 independently of the membrane integrity. The results strengthen the notion that peroxisomes should not be considered as being effective regarding the detoxification of H_2O_2 derived from the surroundings, e.g. mitochondria. In addition, peroxisomes are not able to prevent the release of intra-peroxisomal-derived H_2O_2, despite their high content of catalase. Intact peroxisomes thus represent a potential source of oxidative stress, which might cause damage to the cell or which might modulate redox-sensitive pathways.

Secondly, our findings also have new implications for the understanding of peroxisomal metabolism of fatty acids and other substrates. By determining maximum velocities and Michaelis–Menten constants for several peroxisome oxidases, urate oxidase is found to be the most efficient in generating H_2O_2 in rodents. In addition to urate, glycolate and spermidine, activated fatty acids were also found to be very efficient in generating H_2O_2. The kinetic parameters for H_2O_2 formation in the presence of various fatty acids give rise to several interpretations. Highest β-oxidation rates are found for medium- and long-chain fatty acids [e.g. octanoyl-CoA (C_8) and palmitoyl-CoA (C_{16})]. In fact, the values of K_m and V_{max} are > 10 times higher for octanoyl-CoA compared with lignoceryl-CoA, the longest fatty acid studied (C_{24}). These data suggest an appreciably high capacity of the peroxisomal acyl-CoA oxidase to act on medium-chain fatty acids. This is surprising, since mitochondria are believed to be the main site for β-oxidation [46–49]. Peroxisomes do not oxidize fatty acids that contain less than seven carbons [50,51], and recent studies demonstrate that octanoyl-CoA accumulates during the β-oxidation of longer fatty acids, such as palmitate [52]. Moreover, peroxisomes are considered to metabolize almost exclusively long- and very-long-chain fatty acids [11,50]. Additionally, peroxisomal β-oxidation of long fatty acids is generally believed to yield shorter fatty acids as a direct fuel for mitochondrial β-oxidation. These conclusions have been mainly drawn from the observation that several peroxisome disorders, such as adrenoleukodystrophy, lead to an accumulation of long- and very-long-chain fatty acids [53,54]. Our data suggest that peroxisomes are very capable of contributing to shorter-chain fatty acid oxidation. β-Oxidation of medium-chain fatty acids appears at first glance to be a waste of energy, since oxygen is reduced to water without a concomitant generation of ATP [55]. The (patho)physiological

implications of the β-oxidation of shorter fatty acids, therefore, opens interesting perspectives for future studies.

Thirdly, the real-time measurement of H_2O_2 release from intact peroxisomes provides new insights into the peroxisomal uptake of fatty acids and other substrates. To date, fatty acid transport via the peroxisomal membrane is not completely understood. Long-chain fatty acids are believed to cross the membrane as CoA esters, utilizing fatty-acid transport proteins that were discovered recently [36]. The hydrophilic CoA esters that cannot diffuse through lipid membranes are synthesized at the peroxisomal membrane by acyl-CoA synthases. Our real-time measurement of H_2O_2 reveals that this transport is very efficient, and occurs at a fast rate in the absence of energy-delivering co-substrates, such as ATP. Thus our experimental procedure offers an exciting new opportunity to study the transport of fatty acids and other peroxisomal substrates via the peroxisomal membrane in a sensitive manner: an almost unexplored research field.

The methods presented in this study, allowing a direct determination of H_2O_2 metabolism in peroxisomes, will open up new possibilities in defining the role of peroxisome-derived oxidative stress. Since peroxisomes are essential for life in eukaryotic cells, this method is likely to prove to be a valuable tool in understanding the underlying mechanisms for diseases that are caused by malfunctioning of peroxisomal oxygen metabolism.

We thank Dr D. Fahimi for helpful discussions. The technical assistance of H. Mohr is acknowledged. This work was supported by a grant from the University of Heidelberg.

REFERENCES

1 van den Bosch, H., Schütgens, R. B., Wanders, R. J. and Tager, J. M. (1992) Biochemistry of peroxisomes. Annu. Rev. Biochem. **61**, 57–197

2 Breidenbach, R. W. and Beevers, H. (1967) Association of the glyoxylate cycle enzymes in a novel subcellular particle from castor bean endosperm. Biochem. Biophys. Res. Commun. **27**, 462–469

3 Beevers, H. (1982) Glyoxysomes in higher plants. Annu. Rev. Plant Physiol. **386**, 243–253

4 Wanders, R. J., Barth, P. G., Schutgens, R. B. and Tager, J. M. (1994) Clinical and biochemical characteristics of peroxisomal disorders: an update. Eur. J. Pediatr. **153**, 44–48

5 Reddy, J. K., Azarnoff, D. L. and Hignite, C. E. (1980) Hypolipidaemic hepatic peroxisome proliferators form a novel class of chemical carcinogens. Nature (London) **283**, 397–398

6 Rusyn, I., Rose, M. L., Bojes, H. K. and Thurman, R. G. (2000) Novel role of oxidants in the molecular mechanism of action of peroxisome proliferators. Antioxid. Redox. Signaling **2**, 607–621

7 Spiegelman, B. M. (1998) PPAR-γ: adipogenic regulator and thiazolidinedione receptor. Diabetes **47**, 507–514

8 Lumeng, L. and Crabb, D. W. (2000) Alcoholic liver disease. Curr. Opin. Gastroenterol. **16**, 208–218

9 Chitturi, S. and Farrell, G. C. (2001) Etiopathogenesis of nonalcoholic steatohepatitis. Semin. Liver Dis. **21**, 27–41

10 Rao, M. S. and Reddy, J. K. (2001) Peroxisomal β-oxidation and steatohepatitis. Semin. Liver Dis. **21**, 43–55

11 Singh, I. (1997) Biochemistry of peroxisomes in health and disease. Mol. Cell. Biochem. **167**, 1–29

12 Singh, I. (1996) Mammalian peroxisomes: metabolism of oxygen and reactive oxygen species. Ann. N.Y. Acad. Sci. **804**, 612–627

13 De Duve, C. and Baudhuin, P. (1966) Peroxisomes (microbodies and related particles). Physiol. Rev. **46**, 323–357

14 Cadenas, E. (1989) Biochemistry of oxygen toxicity. Annu. Rev. Biochem. **58**, 79–110

15 Forman, H. J. and Cadenas, E. (1997) Oxidative stress and signal transduction, Chapman and Hall, New York

16 Khan, A. U. and Wilson, T. (1995) Reactive oxygen species as cellular messengers. Chem. Biol. **2**, 437–445

17 Burdon, R. H. (1995) Superoxide and hydrogen peroxide in relation to mammalian cell proliferation. Free Radical Biol. Med. **18**, 775–794

18 Sen, C. K., Sies, H. and Baeuerle, P. A. (2000) Antioxidant and redox regulation of genes, Academic Press, London

19 Meyer, M., Pahl, H. L. and Baeuerle, P. A. (1994) Regulation of the transcription factors NF-κB and AP-1 by redox changes. Chem. Biol. Interact. **91**, 91–100

20 Li, Y., Tharappel, J. C., Cooper, S., Glenn, M., Glauert, H. P. and Spear, B. T. (2000) Expression of the hydrogen peroxide-generating enzyme fatty acyl CoA oxidase activates NF-κB. DNA Cell Biol. **19**, 113–120

21 Mueller, S. and Arnhold, J. (1995) Fast and sensitive chemiluminescence determination of H_2O_2 concentration in stimulated human neutrophils. J. Biolumin. Chemilumin. **10**, 229–237

22 Mueller, S. (2000) Sensitive and non-enzymatic measurement of hydrogen peroxide in biological systems. Free Radical Biol. Med. **29**, 410–415

23 Morris, J. C. (1966) The acid ionization constant of HOCl from 5 to 35 °C. J. Phys. Chem. **70**, 2798–3806

24 Beers, R. F. and Sizer, I. W. (1952) A spectrometric method for measuring the breakdown of hydrogen peroxide by catalase. J. Biol. Chem. **195**, 133–140

25 Volkl, A. and Fahimi, H. D. (1985) Isolation and characterization of peroxisomes from the liver of normal untreated rats. Eur. J. Biochem. **149**, 257–265

26 Volkl, A., Mohr, H. and Fahimi, H. D. (1999) Peroxisome subpopulations of the rat liver. Isolation by immune free flow electrophoresis. J. Histochem. Cytochem. **47**, 1111–1118

27 Crane, D. I., Zamattia, J. and Masters, C. J. (1990) Alterations in the integrity of peroxisomal membranes in livers of mice treated with peroxisome proliferators. Mol. Cell. Biochem. **96**, 153–161

28 Mueller, S., Riedel, D. H. and Stremmel, W. (1997) Determination of catalase activity at physiological H_2O_2 concentrations. Anal. Biochem. **245**, 55–60

29 Laemmli, U. K. (1970) Cleavage of structural proteins during the assembly of the head of bacteriophage T4. Nature (London) **227**, 680–685

30 Angermuller, S. and Fahimi, H. D. (1981) Selective cytochemical localization of peroxidase, cytochrome oxidase and catalase in rat liver with 3,3′-diaminobenzidine. Histochemistry **71**, 33–44

31 Mueller, S., Riedel, H. D. and Stremmel, W. (1997) Direct evidence for catalase as the predominant H_2O_2-removing enzyme in human erythrocytes. Blood **90**, 4973–4978

32 Aebi, H. (1984) Catalase *in vitro*. Methods Enzymol. **105**, 121–126

33 Bright, H. J. and Porter, D. J. (1975) Flavoprotein oxidases. In The enzymes (Boyer, P. D., ed.), pp. 421–503, Academic Press, New York

34 Mueller, S., Pantopoulos, K., Hentze, M. W. and Stremmel, W. (1997) A chemiluminescence approach to study the regulation of iron metabolism by oxidative stress. In Bioluminescence and Chemiluminescence: molecular reporting with photons (Hastings, J. W., Kricka, L. J. and Stanley, P. E., eds.), pp. 338–341, John Wiley & Sons Ltd, Baffins Lane, Chichester

35 Pantopoulos, K., Mueller, S., Atzberger, A., Ansorge, W., Stremmel, W. and Hentze, M. W. (1997) Differences in the regulation of IRP-1 (iron regulatory protein-1) by extra- and intracellular oxidative stress. J. Biol. Chem. **272**, 9802–9808

36 Hettema, E. H. and Tabak, H. F. (2000) Transport of fatty acids and metabolites across the peroxisomal membrane. Biochim. Biophys. Acta **1486**, 18–27

37 Makino, N., Mochizuki, Y., Bannai, S. and Sugita, Y. (1994) Kinetic studies on the removal of extracellular hydrogen peroxide by cultured fibroblasts. J. Biol. Chem. **269**, 1020–1025

38 Chu, R., Varanasi, U., Chu, S., Lin, Y., Usuda, N., Rao, M. S. and Reddy, J. K. (1995) Overexpression and characterization of the human peroxisomal acyl-CoA oxidase in insect cells. J. Biol. Chem. **270**, 4908–4915

39 Chu, R., Lin, Y., Reddy, K. C., Pan, J., Rao, M. S., Reddy, J. K. and Yeldandi, A. V. (1996) Transformation of epithelial cells stably transfected with H_2O_2-generating peroxisomal urate oxidase. Cancer Res. **56**, 4846–4852

40 Kasai, H., Okada, Y., Nishimura, S., Rao, M. S. and Reddy, J. K. (1989) Formation of 8-hydroxydeoxyguanosine in liver DNA of rats following long-term exposure to a peroxisome proliferator. Cancer Res. **49**, 2603–2605

41 Qu, B., Li, Q. T., Wong, K. P., Ong, C. N. and Halliwell, B. (1999) Mitochondrial damage by the 'pro-oxidant' peroxisomal proliferator clofibrate. Free Radical Biol. Med. **27**, 1095–1102

42 Cattley, R. C. and Glover, S. E. (1993) Elevated 8-hydroxydeoxyguanosine in hepatic DNA of rats following exposure to peroxisome proliferators: relationship to carcinogenesis and nuclear localization. Carcinogenesis **14**, 2495–2499

43 Mueller, S., Pantopoulos, K., Hubner, C. A., Stremmel, W. and Hentze, M. W. (2001) IRP1 activation by extracellular oxidative stress in the perfused rat liver. J. Biol. Chem. **276**, 23192–23196

44 Test, S. T. and Weiss, S. J. (1984) Quantitative and temporal characterization of the extracellular H_2O_2 pool generated by human neutrophils. J. Biol. Chem. **259**, 399–405

45 Nicholls, P. (1965) Activity of catalase in the red cell. Biochim. Biophys. Acta **99**, 286–297

46 Kerner, J. and Hoppel, C. (2000) Fatty acid import into mitochondria. Biochim. Biophys. Acta **1486**, 1–17

47 Debeer, L. J. and Mannaerts, G. P. (1983) The mitochondrial and peroxisomal pathways of fatty acid oxidation in rat liver. Diabetes Metab. **9**, 134–140
48 Mannaerts, G. P., Debeer, L. J., Thomas, J. and De Schepper, P. J. (1979) Mitochondrial and peroxisomal fatty acid oxidation in liver homogenates and isolated hepatocytes from control and clofibrate-treated rats. J. Biol. Chem. **254**, 4585–4595
49 Kondrup, J. and Lazarow, P. B. (1985) Flux of palmitate through the peroxisomal and mitochondrial β-oxidation systems in isolated rat hepatocytes. Biochim. Biophys. Acta **835**, 147–153
50 Lazarow, P. B. (1978) Rat liver peroxisomes catalyze the beta oxidation of fatty acids. J. Biol. Chem. **253**, 1522–1528
51 Osumi, T. and Hashimoto, T. (1978) Acyl-CoA oxidase of rat liver: a new enzyme for fatty acid oxidation. Biochem. Biophys. Res. Commun. **83**, 479–485
52 Hashimoto, F., Furuya, Y. and Hayashi, H. (2001) Accumulation of medium chain acyl-CoAs during β-oxidation of long chain fatty acid by isolated peroxisomes from rat liver. Biol. Pharm. Bull. **24**, 600–606
53 Forss-Petter, S., Werner, H., Berger, J., Lassmann, H., Molzer, B., Schwab, M. H., Bernheimer, H., Zimmermann, F. and Nave, K. A. (1997) Targeted inactivation of the X-linked adrenoleukodystrophy gene in mice. J. Neurosci. Res. **50**, 829–843
54 Singh, I., Lazo, O., Dhaunsi, G. S. and Contreras, M. (1992) Transport of fatty acids into human and rat peroxisomes. Differential transport of palmitic and lignoceric acids and its implication to X-adrenoleukodystrophy. J. Biol. Chem. **267**, 13306–13313
55 Lazarow, P. B. (1982) Compartmentation of β-oxidation of fatty acids in peroxisomes. In Metabolic Compartmentation (Sies, H., ed.), pp. 317–329, Academic Press, New York

Received 14 October 2001/24 January 2002; accepted 12 February 2002